Hyperelasticity and Stress Softening of Filler Reinforced Polymer Networks

Manfred Klüppel

Deutsches Institut für Kautschuktechnologie e. V., Eupener Str. 33,
30519 Hannover, Germany
Email: manfred.klueppel@DIKautschuk.de

Summary: Starting from an analysis of filler networking in bulk polymers, a constitutive micro-mechanical model of stress softening and hysteresis of filler reinforced polymer networks is developed. It refers to a non-affine tube model of rubber elasticity, including hydrodynamic amplification of the rubber matrix by a fraction of hard, rigid filler clusters with filler-filler bonds in the unbroken, virgin state. The filler-induced hysteresis is described by an anisotropic free energy density, considering the cyclic breakdown and re-aggregation of the residual fraction of soft filler clusters with already broken, damaged filler-filler bonds. Experimental investigations of the quasi-static stress-strain behaviour of silica and carbon black filled rubbers up to large strain agree well with adaptations found by the developed model. The microscopic material parameters obtained appear reasonable, providing information on the mean size and distribution width of filler clusters, the tensile strength of filler-filler bonds and the polymer network chain density.

Keywords: elastomers; filler networking; hysteresis; stress softening; tube model

Introduction

Despite a high technological interest, the micro-mechanical background of filler reinforcement of elastomers is still an unsolved problem. Here, a constitutive model of hyperelasticity and stress softening of filler-reinforced polymer networks is presented that is based on a molecular-statistical theory of rubber elasticity[1-3] and a micro-mechanical concept of filler cluster breakdown in strained elastomer composites.[4-6] We will first give a short review of the extended tube model used for modelling the elasticity of the polymer matrix. Then we will focus on the viscoelastic response of hard and soft filler clusters in elastomer composites. Finally, the model is adapted to stress-strain curves of unfilled and filled polymer networks up to large strain, where a simultaneous fit to the case of uniaxial and equi-biaxial deformations is achieved.

© 2003 WILEY-VCH Verlag GmbH & KGaA, Weinheim DOI: 10.1002/masy.200351004

The Extended Tube Model of Rubber Elasticity

The well known non-linear elastic response of stretched polymer networks is most basically described by a tube model of rubber elasticity. It takes into account that the network chains in a highly entangled polymer network are heavily restricted in their fluctuations due to packing effects. These restrictions are described by virtual tubes around the network chains. When the network elongates, the tubes deform less than affinely with a deformation exponent $\nu = 1/2$. It means that the tube radius d_μ in spatial direction μ of the main axis system depends on the deformation ratio λ_μ as follows:[1]

$$d_\mu = d_o \, \lambda_\mu^{\nu} \tag{1}$$

where d_o is the tube radius in the non-deformed state. Experimental evidence of non-affine tube deformations according to Eq. (1) is provided by neutron scattering of strained rubbers[7] as well as stress-strain measurements on swollen polymer networks.[8]

The non-affine tube model was originally derived for the case of Gaussian chain statistics.[1] For applications up to large strains, we take into account that the network chains have a finite length and stress in the network becomes infinitely large when the chains between two subsequent network junctions are stretched fully. Then, the free energy density of the extended, non-Gaussian tube model with non-affine tube deformation is obtained as:[3-6,9,10]

$$W_R = \frac{G_c}{2}\left\{\frac{\left(\sum_{\mu=1}^{3}\lambda_\mu^2 - 3\right)\left(1 - \frac{T_e}{n_e}\right)}{1 - \frac{T_e}{n_e}\left(\sum_{\mu=1}^{3}\lambda_\mu^2 - 3\right)} + \ln\left[1 - \frac{T_e}{n_e}\left(\sum_{\mu=1}^{3}\lambda_\mu^2 - 3\right)\right]\right\} + 2G_e\left(\sum_{\mu=1}^{3}\lambda_\mu^{-1} - 3\right) \tag{2}$$

Here, n_e is the number of statistical chain segments between two subsequent entanglements and T_e is the trapping factor ($0<T_e<1$), which characterizes the portion of elastically active entanglements. The first bracket term of Eq. (2) describes the constraints due to inter-chain junctions, with an elastic modulus G_c proportional to the density of network junctions, i.e., cross-links and trapped entanglements. The second addend considers the topological tube constraints, whereby G_e is proportional to the entanglement density μ_e of the rubber. The parenthetical expression in the first addend takes into account the finite chain extensibility.[2] For the limiting case $n_e/T_e = \sum \lambda_\mu^2 - 3$, the free energy density Eq. (2) exhibits a singularity, which is reached when the chains between successive trapped entanglements are stretched

© 2003 WILEY-VCH Verlag GmbH & KGaA, Weinheim

fully. For the moduli G_c and G_e, the following relations to molecular material parameters hold:

$$G_c = A_c \, \nu_{mech} \, k_B T \tag{3}$$

$$G_e = \frac{\rho \, N_a \, l_s^2 \, k_B T}{4\sqrt{6} \, M_s \, d_o^2} \tag{4}$$

Here, ν_{mech} is the mechanically effective chain density (specified e.g., in Ref. [3]), A_c is a micro-structure factor that describes the fluctuations of network junctions, N_a the Avogadro number, ρ the mass density, M_s and l_s the molar mass and length of the statistical segments, respectively, k_B the Boltzmann constant and T the absolute temperature. The microstructure factor $A_c = 1$ if the cross-link fluctuations are totally suppressed and $A_c = 1/2$ for freely fluctuating tetrafunctional cross-links of a phantom network. In the present case of tetrafunctional network junctions consisting of cross-links and trapped entanglements, $A_c \approx 0.67$.[11]

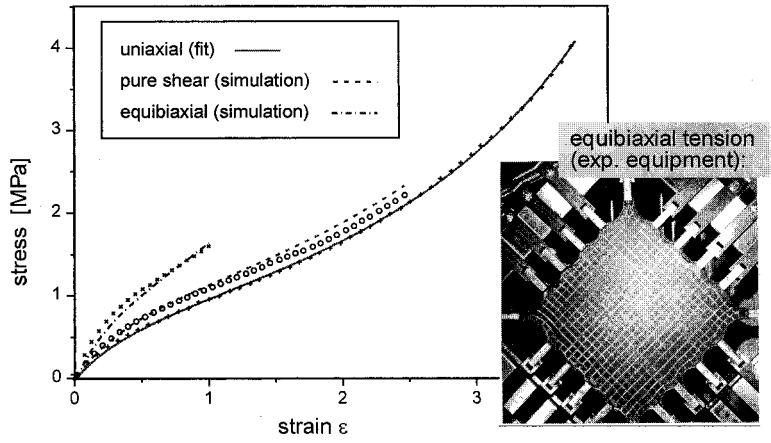

Fig. 1. Stress-strain data (symbols) and simulation curves (lines) of an unfilled NR for three deformation modes, as indicated. The material parameters are obtained from a fit to the uniaxial data: G_c = 0.43 MPa, G_e = 0.20 MPa and n_e/T_e =68. The inset shows a photograph of the experimental equipment used for the equi-biaxial measurements.

The validity of this model is tested in Fig. 1, where the apparent stress $\sigma_{R,\mu} = \partial W_R / \partial \lambda_\mu$. in spatial direction μ is fitted to stress-strain data of an unfilled NR-vulcanizate for three different deformation modes. Thereby, a single set of material parameters G_c, G_e and n_e/T_e has been used that have been found from a fit to the uniaxial data. Obviously, the model gives a good fit to the

© 2003 WILEY-VCH Verlag GmbH & KGaA, Weinheim

uniaxial data up to large strain. Furthermore, the obtained material parameters also provide a fair prediction for the two other deformation modes. The observed deviations are within the range of experimental errors.

It must be pointed out that the material parameter G_e can be determined in principle more precisely by means of equi-biaxial measurements than by uniaxial measurements, since, contrary to the uniaxial case, the G_e-term increases (almost linearly) with λ, owing to the strong lateral contraction on equi-biaxial extension. This implies a close dependency of the equi-biaxial stress on the tube constraint modulus, since G_c and G_e contribute nearly equally to the stress, also at large strain. For uniaxial extensions this is not the case, but the tube constraints lead to significant effects only in the medium strain regime. The stress at large strain is governed by the G_c-term. Accordingly, a comparative study of uniaxial- and equi-biaxial extension modes allows for a test of the tube deformations in strained polymer networks. So far, the agreement between experimental data and fits for the different deformation modes (Fig. 1) provides another indirect proof of the non-affine tube deformation law Eq. (1). Obviously, the model passes this "plausibility criterion".

We finally note that the value of the tube constraint modulus is closely related to the dynamic plateau modulus G_N^o, since both moduli vary linearly with the density of entanglements and the relationship $G_e \approx (1/2)\ G_N^o$ holds. Accordingly, the parameter G_e is not necessarily a fit parameter but rather it is specified by the microstructure of the polymer. Obviously, the fit value $G_e = 0.2$ MPa obtained in Fig. 1 is in fair agreement with the above relation, since $G_N^o \approx 0.58$ MPa holds for uncross-linked NR-melts.[12] In the next section, where the extended tube model is applied to filler reinforced polymer networks, we will consider G_e as fixed parameter determined by $G_e \approx (1/2)\ G_N^o$.

Stress Softening and Filler-induced Hysteresis

Reinforcement of polymer networks by nano-structured fillers like carbon blacks or silica is assumed to be related to the presence of physically bonded, fractal filler clusters in the rubber matrix that exhibit a particular size distribution $\phi(\xi_\mu)$. With increasing strain of a virgin sample, a successive breakdown of the filler clusters takes place under the exposed stress of the bulk polymer network. This begins with the largest clusters and continues up to a minimum cluster size ξ_{min}, which is specified below (Eq. (14)). During the back-cycle, re-aggregation of the

© 2003 WILEY-VCH Verlag GmbH & KGaA, Weinheim

filler particles takes place, but the damaged filler-filler bonds that are formed after once being broken differ from the original virgin ones. Since in general the virgin bonds are annealed by the heat treatment during vulcanization,[4] the damaged bonds are significantly softer and more fragile than the original ones. This mechanism implies a pronounced stress softening of the pre-strained samples, since hard cluster units are replaced by soft ones. Furthermore, in subsequent stress-strain cycles the re-aggregated filler clusters with soft bonds bend substantially in the stress field of the rubber, implying that a certain amount of energy is stored in the clusters, which is dissipated when the clusters break. This mechanism leads to a filler-induced viscoelastic contribution to the total stress that impacts the internal friction or hysteresis of filled polymer networks, significantly. It is important to note that this kind of viscoelastic response is present also in the limit of quasi-static deformations, where no explicit time dependency of the stress-strain cycles is considered.

According to this scenario, two micro-mechanical mechanisms of cyclically strained reinforced polymer networks are distinguished. On the one side, stress softening is considered to be related to hydrodynamic reinforcement of the rubber matrix by a fraction of hard filler clusters with strong filler-filler bonds in the virgin, annealed state. On the other hand, filler induced hysteresis results from a cyclic breakdown and re-aggregation of the residual fraction of more fragile filler clusters with softer, already damaged filler-filler bonds. The fraction of rigid filler clusters decreases with increasing pre-strain, while the fraction of fragile filler clusters increases. This leads to a shift of the boundary size ξ_{min} with increasing pre-strain. The decomposition into hard and soft filler cluster units is depicted in Fig. 2.

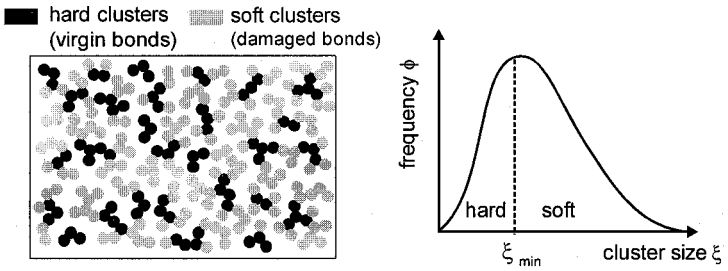

Fig. 2. Schematic view of the decomposition of filler clusters into hard and soft units for pre-conditioned samples. The right hand side shows the cluster size distribution with the pre-strain dependent boundary size ξ_{min}.

© 2003 WILEY-VCH Verlag GmbH & KGaA, Weinheim

Accordingly, we assume that for quasi-static, cyclic deformations of filler reinforced rubbers up to large strain the total free energy density consists of two contributions:

$$W(\varepsilon_\mu) = W_R(\varepsilon_\mu) + W_A(\varepsilon_\mu) \tag{5}$$

The first addend considers the equilibrium energy density Eq. (2) of the strained rubber matrix, including hydrodynamic reinforcement by the fraction of rigid filler clusters, as specified below. The second addend describes the energy stored in the substantially strained soft, fragile filler clusters:

$$W_A(\varepsilon_\mu) = \sum_{\mu}^{\dot{\varepsilon}_\mu > 0} \frac{1}{2d} \int_{\xi_{\mu,\min}}^{\xi_\mu(\varepsilon_\mu)} G_A\left(\xi'_\mu\right) \varepsilon^2_{A,\mu}\left(\xi'_\mu, \varepsilon_\mu\right) \phi\left(\xi'_\mu\right) d\xi'_\mu \tag{6}$$

Here, d is the particle size and ξ_μ is the cluster size in spatial direction μ of the main axis system. $\phi(\xi_\mu)$ is the normalized size distribution of the clusters that is considered to be isotropic, i.e., $\phi(\xi_1) = \phi(\xi_2) = \phi(\xi_3)$. G_A is the elastic modulus and $\varepsilon_{A,\mu}$ is the strain of the fragile filler clusters.

The dot appearing in the upper limit of the sum in Eq. (6) denotes time derivative, which means that the sum is taken over stretching directions with $\partial\varepsilon_\mu/\partial t > 0$, only. Consequently, clusters are strained and successively broken in stretching directions alone. Healing of the clusters takes place in the compression directions, implying that a cyclic breakdown and re-aggregation of clusters can be described. The integration in Eq. (6) is performed over the fraction of fragile filler clusters with a cluster size lying in the interval $\xi_{\mu,\min} < \xi_\mu < \xi_\mu(\varepsilon_\mu)$, which are not broken at exposed strain ε_μ of the actual cycle.

The clusters smaller than $\xi_{\mu,\min}$, representing the fraction that survived the maximum exposed pre-strain $\varepsilon_{\mu,\max}$ in a previous deformation cycle, are assumed to dominate the hydrodynamic reinforcement of the rubber matrix. Due to the stiff nature of their filler-filler bonds, corresponding to the bonds in the virgin state of the sample, these clusters can considered to behave quite rigidly. Accordingly, the contribution of the stiff clusters to the stored energy of the clusters W_A is neglected. Their mechanical action refers to an overstraining of the rubber matrix, which is quantified by a strain amplification factor X. It relates the external strain ε_μ of the sample to the internal strain ratio λ_μ of the rubber matrix:

$$\lambda_\mu = 1 + X\,\varepsilon_\mu \tag{7}$$

© 2003 WILEY-VCH Verlag GmbH & KGaA, Weinheim

For the first deformation of virgin samples the strain amplification factor depends on the external strain ($X = X(\varepsilon_\mu)$).In the case of a pre-strained sample and for strains smaller than the previous straining ($\varepsilon_\mu < \varepsilon_{\mu,max}$), it is constant and determined by $\varepsilon_{\mu,max}$ ($X = X(\varepsilon_{\mu,max})$).

In the following we apply a relation considering the strain amplification factor of overlapping fractal clusters (high filler concentrations), as derived by Huber and Vilgis.[13,14] In the present case, the amplification factors $X(\varepsilon_\mu)$ and $X(\varepsilon_{\mu,max})$ are evaluated by averaging over the size distribution of rigid clusters in all space directions. For pre-strained samples this yields:

$$X(\varepsilon_{\mu,max}) = 1 + c\left(\frac{\Phi}{\Phi_p}\right)^{\frac{2}{3-d_f}} \sum_{\mu=1}^{3} \frac{1}{d} \int_0^{\xi_{\mu,min}} \left(\frac{\xi'_\mu}{d}\right)^{d_w - d_f} \phi\left(\xi'_\mu\right) d\xi'_\mu \qquad (8)$$

Here, c is a constant of order one, Φ is the filler volume fraction and Φ_p is the solid fraction of the filler particles that differs from the ideal value $\Phi_p = 1$ in the case of non-spherical, structured filler particles. d_f is the fractal dimension and d_w is the anomalous diffusion exponent on fractal clusters. For the case of virgin samples, $X(\varepsilon_\mu)$ is obtained in a similar way by performing the integration in Eq. (8) from zero up to the strain dependent cluster size $\xi_\mu(\varepsilon_\mu)$, which will be specified below.

The elastic modulus G_A of the clusters, appearing in Eq. (6), can be evaluated by referring to the Kantor-Webman model of flexible, curved chain aggregates.[15] In a simplified approach introduced by Lin and Lee,[16] the contributions from the two different kinds of angular deformation, bending and twisting, can be considered by an averaged bending-twisting deformation. This is obtained by replacing the elastic bending constant G through an averaged elastic constant $\overline{G}$. It yields:

$$G_A \equiv \xi^{-1} k_S = \frac{\kappa \overline{G}}{d^3} \left(\frac{d}{\xi}\right)^{3+d_{f,B}} \qquad (9)$$

where κ is a geometrical factor of order one and $d_{f,B}$ is the backbone fractal dimension of the filler clusters. For large clusters, the force constant $k \approx k_S$ of the cluster backbone is found as:

$$k_S = \frac{\kappa \overline{G}}{d^2} \left(\frac{d}{\xi}\right)^{2+d_{f,B}} \qquad (10)$$

Eq. (9) describes the modulus G_A of the clusters as a local elastic bending-twisting energy term $\overline{G}$ times a scaling function that involves the size and geometrical structure of the clusters. In

© 2003 WILEY-VCH Verlag GmbH & KGaA, Weinheim

the special case of a linear cluster backbone with $d_{f,B} = 1$, Eqs. (9) and (10) correspond to the well known elastic behaviour of linear, flexible rods. In this case, the bending modulus falls off with the 4th power of the rod length and the force constant decreases as the 3rd power. The above approach represents a generalization of this behaviour to the case of flexible, curved rods.

For estimating the limiting cluster size $\xi_{\mu,min}$ as a function of external strain ε_μ, the ultimate properties of fractal filler clusters have to be described on a microscopic level. The failure- or yield strain ε_F of the filler clusters results from the fact that a single cluster corresponds to a series of two molecular springs: a soft one, representing the bending-twisting mode, and a stiff one, representing the tension mode. On the one hand, the soft spring with force constant $k_S \sim \overline{G}$ affects the elasticity of the whole system, since in general the deformation of the stiff spring can be neglected (Eqs. (9), (10)). On the other hand, the stiff spring governs the fracture behaviour of the system, because it considers the longitudinal deformation and hence, spatial separation of filler-filler bonds. Fracture of the cluster takes place, when a critical separation of bonded filler particles is exceeded and the failure strain ε_b of filler-filler bonds is reached. The mechanical equivalence between filler clusters and a series of two springs is illustrated in Fig. 3.

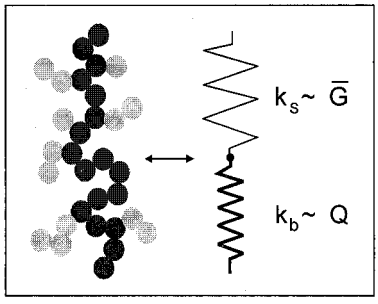

Fig. 3. Schematic view demonstrating the mechanical equivalence between a filler cluster and a series of soft and stiff molecular springs, representing the bending-twisting- and tension deformation of filler-filler bonds, respectively.

© 2003 WILEY-VCH Verlag GmbH & KGaA, Weinheim

The failure strain ε_F of the filler cluster can be evaluated from the stress equilibrium between the two springs. With Eq. (10) one finds in the case of large clusters with $k_b >> k_S$:

$$\varepsilon_F = \left(1+\frac{k_b}{k_s}\right)\varepsilon_b \approx \frac{Q\varepsilon_b}{\kappa \overline{G}}\left(\frac{\xi}{d}\right)^{2+d_{f,B}} \tag{11}$$

Here, Q is the elastic tension constant of the Kantor-Webman model and $k_b = Q/d^2$ is the force constant of longitudinal deformations of filler-filler bonds.[15] Eq. (11) implies that the yield strain of a filler cluster increases with the cluster size ξ according to a power law. Furthermore, it is governed by the ratio of the elastic constants $Q/\overline{G}$. Consequently, larger clusters show a higher extensibility than smaller ones, due to the ability to bend and twist around the bonds and the clusters can survive up to large strain due to their high flexibility in strained rubbers. This kind of elastic behaviour and the dependence of strength on cluster size plays a crucial role in stress softening and filler-induced hysteresis up to large strain.

Finally, to analyse the fracture behaviour of filler clusters in strained polymer networks, we have to evaluate the strain $\varepsilon_{A,\mu}$ of the filler clusters relative to the external strain ε_μ of the sample. At medium and large strains, when a stress induced gel-sol transition of the pervading filler network has taken place (for $\varepsilon >$ about 5%), the stress on the filler clusters is transmitted by the rubber matrix. Then, $\varepsilon_{A,\mu}$ follows from the stress equilibrium between the clusters and the rubber matrix ($\varepsilon_{A,\mu} G_A(\xi_\mu) = \hat{\sigma}_{R,\mu}(\varepsilon_\mu)$). This yields with Eq. (9):

$$\varepsilon_{A,\mu}(\varepsilon_\mu) = \frac{d^3}{\kappa \overline{G}}\left(\frac{\xi_\mu}{d}\right)^{3+d_{f,B}} \hat{\sigma}_{R,\mu}(\varepsilon_\mu) \tag{12}$$

Here, $\hat{\sigma}_{R,\mu}(\varepsilon_\mu)$ is the norm of the relative stress of the rubber matrix related to the initial stress at the beginning of each strain cycle, where $\partial\varepsilon_\mu/\partial t = 0$:

$$\hat{\sigma}_{R,\mu}(\varepsilon_\mu) \equiv \left|\sigma_{R,\mu}(\varepsilon_\mu) - \sigma_{R,\mu}(\partial\varepsilon_\mu/\partial t = 0)\right| \tag{13}$$

The application of this normalized, relative stress in the stress equilibrium Eq. (12) is essential for a constitutive formulation of cyclic cluster breakdown and re-aggregation during every stress-strain cycle. It makes sure that the clusters are never compressed but only stretched in spatial directions with $\partial\varepsilon_\mu/\partial t > 0$, since $\varepsilon_{A,\mu} \geq 0$ holds owing to the norm in Eq. (13). In the

© 2003 WILEY-VCH Verlag GmbH & KGaA, Weinheim

compression directions with $\partial\varepsilon_\mu / \partial t < 0$ re-aggregation of the filler particles takes place, which is not specified here. This will be the task of future investigations, since a complete description of any kind of hysteresis cycle requires an understanding of re-aggregation, as well.

By comparing Eqs. (11) and (12) one finds that the strain $\varepsilon_{A,\mu}$ of the clusters increases faster with their size ξ_μ then the failure strain $\varepsilon_{F,\mu}$. Accordingly, with increasing strain the large clusters in the system break first, followed by the smaller ones. The maximum size ξ_μ of clusters surviving at exposed external strain ε_μ is found from the stress equilibrium between the rubber matrix and the failure stress $\sigma_{F,\mu}$ of the clusters ($\sigma_{F,\mu} = \varepsilon_{F,\mu}\, G_A(\xi_\mu)$):

$$\xi_\mu(\varepsilon_\mu) = \frac{Q\varepsilon_b}{d^2\,\hat{\sigma}_{R,\mu}(\varepsilon_\mu)} \tag{14}$$

This allows for an evaluation of the boundaries of the integrals in Eqs. (6) and (8). Hence, the nominal stress contribution of the stretched filler clusters can be calculated. They are determined by $\sigma_{A,\mu} = \partial W_A/\partial\varepsilon_{A,\mu}$, where the sum over all stretching directions, that differ for the up- and down cycle, has to be considered. For uniaxial deformations $\varepsilon_1 = \varepsilon$, $\varepsilon_2 = \varepsilon_3 = (1+\varepsilon)^{-1/2}$-1 one obtains a positive contribution to the total nominal stress in the stretching direction for the up-cycle:

$$\sigma_{0,1}^{up}(\varepsilon) = \sigma_{R,1}(\varepsilon) + \hat{\sigma}_{R,1}(\varepsilon) \int_{\frac{Q\varepsilon_b}{d^3\hat{\sigma}_{R,1}(\varepsilon_{max})}}^{\frac{Q\varepsilon_b}{d^3\hat{\sigma}_{R,1}(\varepsilon)}} \phi(x_1)\, dx_1 \tag{15}$$

with the abbreviations:

$$\hat{\sigma}_{R,1}(\varepsilon) = \left|\sigma_{R,1}(\varepsilon) - \sigma_{R,1}(\varepsilon_{min})\right| \tag{16}$$

and $x_1 = \xi_1/d$. For the down-cycle in the same direction one finds a negative contribution to the total stress due to the norm in Eq. (13):

$$\sigma_{0,1}^{down}(\varepsilon) = \sigma_{R,1}(\varepsilon) - 2\tilde{\sigma}_{R,1}(\varepsilon) \int_{\frac{Q\varepsilon_b(1+\varepsilon_{min})^{-3/2}}{2d^3\tilde{\sigma}_{R,1}(\varepsilon_{min})}}^{\frac{Q\varepsilon_b(1+\varepsilon)^{-3/2}}{2d^3\tilde{\sigma}_{R,1}(\varepsilon)}} \phi(x_1)dx_1 \tag{17}$$

© 2003 WILEY-VCH Verlag GmbH & KGaA, Weinheim

The negative stress contribution results from the stretching of clusters in the lateral direction that hinders the relaxation of the polymer network during the back-cycle. In Eq. (17), the abbreviation:

$$\tilde{\sigma}_{R,l}(\varepsilon) = \left| \sigma_{R,l}(\varepsilon) - \left(\frac{1+\varepsilon_{max}}{1+\varepsilon} \right)^{3/2} \sigma_{R,l}(\varepsilon_{max}) \right| \tag{18}$$

has been used. The different choices of the extrema with $\partial\varepsilon_\mu/\partial t = 0$ in Eq. (16) and (18) are due to the fact that an up-cycle begins at $\varepsilon = \varepsilon_{min}$, but a down-cycle begins at $\varepsilon = \varepsilon_{max}$. As a rule, the relative stresses in the lower boundaries of the integrals in Eqs. (15) and (17) have to be chosen in such a way that they attain their maximum values, implying that all fragile clusters are broken and the condition $\xi_\mu = \xi_{\mu,min}$ holds. Note that stress-strain cycles starting or ending at an intermediate strain between ε_{max} and ε_{min} cannot be described by the present model, since the re-aggregation mechanism is not considered so far.

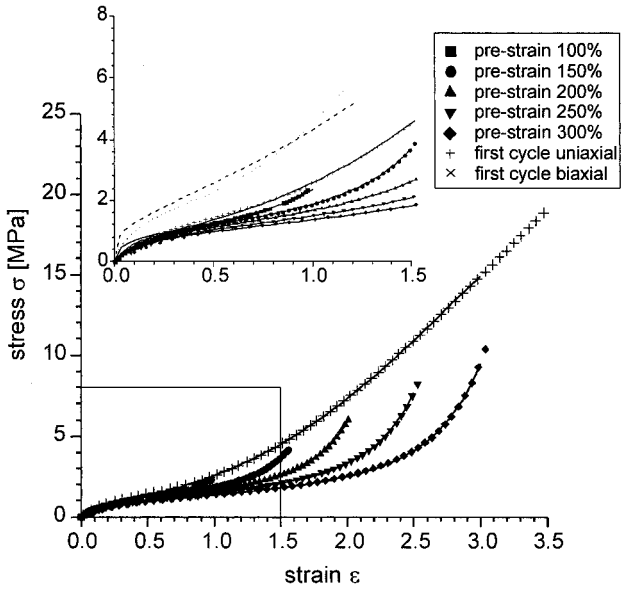

Fig. 4. Uniaxial stress softening data (symbols) of a carbon black filled S-SBR sample at various pre-strains. The insert shows a magnification at small strains, also including equi-biaxial data for the first stretching cycle. The lines are simulation curves (Eq. (15)) with the log-normal cluster size distribution Eq. (19).

© 2003 WILEY-VCH Verlag GmbH & KGaA, Weinheim

Fig. 4 shows a fit of the developed model for the up-cycles (Eq. (15)) to experimental stress-strain data of a carbon black filled S-SBR-sample at different pre-strains. Thereby, a logarithmic normal cluster size distribution function $\phi(x_1)$, with the abbreviation $x_1 = \xi_1/d$, has been chosen:

$$\phi(x_1) = \frac{\exp\left(-\frac{\ln(x_1 / < x_1 >)^2}{2b^2}\right)}{\sqrt{\pi/2}\, b\, x_1} \tag{19}$$

As demonstrated in Fig. 4, a very good adaptation for the pre-conditioned samples can be obtained with a single set of polymer parameters (G_c = 0.176 MPa, G_e = 0.2 MPa, n_e/T_e = 100), simply by varying the strain amplification factor X. The fitted parameters are X_i = 4.90; 3.83; 3.22; 2.71; 2.34 for pre-strain increasing successively from ε_{max} = 100 to 300 %. Further fit parameters are the yield stress of filler-filler bonds $Q\varepsilon_b/d^3$ = 26 MPa as well as the relative mean cluster size $<x_1>$ = 25 and distribution width b = 0.8.

The above set of fit parameters $X_i(\varepsilon_{max})$ appears appropriate for an estimation of the strain dependency of the amplification factor $X(\varepsilon)$, which is needed for a simulation of the stress-strain behaviour of the virgin samples. Unfortunately, a simple fit with Eq. (8) is not possible, because the upper boundary of the integral $\xi_\mu(\varepsilon)$ depends on $X(\varepsilon)$ itself (Eq. (14)) and a general analytical solution of the integral in Eq. (8) is not known. For that reason an empirical power law dependency of the amplification factor X on a scalar strain variable E, involving the first deformation invariant $I_1(\varepsilon_\mu)$, is applied:

$$X(E) = X_\infty + (X_o - X_\infty)(1+E)^{-y} \tag{20}$$

Thereby, the strain variable:

$$E(\varepsilon_\mu) \equiv \left(\sum_{\mu=1}^{3}(1+\varepsilon_\mu)^2 - 3\right)^{1/2} \tag{21}$$

has been used for the fit to the X_i-values. It yields X_∞ = -1.21 and X_o = 11.5 for the limiting strain amplification factors at infinite and zero strain, respectively, and y =0.8 as an empirical exponent. With these values, the simulation of the first uniaxial stretching cycle of the virgin sample shown in Fig. 4 fits very well to the experimental data. Furthermore, a fair simulation is also obtained for the equi-biaxial measurement data, as shown in the inset of Fig. 4. This

© 2003 WILEY-VCH Verlag GmbH & KGaA, Weinheim

implies that the "plausibility criterion", discussed at the end of Section 2, is also fulfilled for the stress softening model of filler reinforced rubbers.

Conclusions and Outlook

From the fair agreement between simulation curves and experimental stress-strain data for the different deformation modes it can be concluded that the extended tube together with the model of cluster breakdown and re-aggregation represents a fundamental micro-mechanical basis for the description of stress softening and non-linear viscoelasticity of filler reinforced polymer networks. In this way, the mechanisms of energy storage and dissipation are traced back to the elastic response of the polymer network as well as the elasticity and fracture properties of flexible filler clusters. For a complete, time dependent, characterization of non-linear viscoelastic stress-strain cycles of filler reinforced polymer networks, the dynamic-mechanical response of the polymer matrix has to be considered, as well. Furthermore, the re-aggregation rate must be specified in dependence of strain, in order to describe any kind of stress-strain cycles. This will be a task of future work.

[1] G. Heinrich, E. Straube, G. Helmis, *Adv. Polym. Sci.* **1988**, *85*, 33.
[2] S. F. Edwards, T. A. Vilgis, *Rep. Prog. Phys.* **1988**, *51*, 243; *Polymer* **1986**, *27*, 483.
[3] M. Klüppel, H. Menge, H. Schmidt, H. Schneider, R. H. Schuster, *Macromolecules* **2001**, *34*, 8107.
[4] M. Klüppel, *Adv. Polym. Sci.*, in press
[5] M. Klüppel, J. Schramm, Macromol. Theory Simul. **2000**, *9*, 742.
[6] M. Klüppel, J. Meier, in: "*Constitutive Models for Rubber II*", D. Besdo, R. H. Schuster, J. Ihlemann, Eds., A. A. Balkema, Lisse, Abingdon, Exton, Tokyo, 2001, p. 11.
[7] E. Straube, V. Urban, W. Pyckhout-Hintzen, D. Richter, C. W. Glinka, *Phys. Rev. Lett.* **1995**, *74*, 4464.
[8] M. Klüppel, *Macromolecules* **1994**, *27*, 7179.
[9] M. Kaliske, G. Heinrich, *Rubber Chem. Technol.* **1999**, *72*, 602.
[10] G. Heinrich, M. Kaliske, *Computational and Theoretical Polym. Sci.* **1997**, *7*, 227.
[11] M. Klüppel, G. Heinrich, *Macromolecules* **1994**, *27*, 3569.
[12] L. J. Fetters, D. J. Lohse, D. Richter, T. A. Witten, A. Zirkel, *Macromolecules* **1994**, *27*, 4639.
[13] G. Huber, PhD-Thesis, University Mainz, Germany, 1997.
[14] G. Huber, T. A. Vilgis, *Euro. Phys. J.* **1998**, *B3*, 217; *Kautschuk Gummi Kunstst.* **1999**, *52*, 102.
[15] Y. Kantor, I. Webman, *Phys. Rev. Lett.* **1984**, *52*, 1891.
[16] C.-R. Lin, Y.-D. Lee, *Macromol. Theory Simul.* **1996**, *5*, 1075; *ibid.* **1997**, *6*, 102.

© 2003 WILEY-VCH Verlag GmbH & KGaA, Weinheim